LIMITED

THE UNIVERSITY OF MICHIGAN

3727-1-F

RADAR CROSS SECTION INVESTIGATION

FOR THE

BOEING AIRPLANE COMPANY

by

J.W. Crispin Jr. and R.E. Hiatt

August 1960

Purchase Order No. 295353

Prepared for:

Boeing Airplane Co.

Witchita, Kansas

LIMITED

TABLE OF CONTENTS

I. INTRODUCTION

On 13 June 1960 a radar cross section investigation was begun for the Boeing Airplane Company (Wichita, Kansas) under Boeing Airplane Company Purchase Order No. 295353. The program of study is outlined in Boeing document No. D3-3077. Briefly the program consisted of a study of the radar cross section characteristics of three models which were defined in D3-3077 as follows:

Model "A" - Model "A" to be a model in the general configuration of an airplane having a wing span of approximately $21\frac{1}{2}$ inches and a fuselage length of 32 inches.

Model "B" - Model "B" to have the same dimensions as Model "A" but will differ slightly in configuration.

Model "C" - Model "C" will be a geometrical construction resembling two spheroids connected by a long cylinder.

In fact "A" was an "airplane" having a cylindrical fuselage and straight wings while "B" had a curved fuselage and curved wings. Figure 1-1 contains photographs of the three models.

Experimental measurements were made on these three models at 2870 mcs, 9800 mcs and 22.96 kmcs. Since these models are 1/10-scale models of the actual configurations of interest, this gave "full-scale" data at 287, 980, and 2296 mcs. All measurements were made in the plane containing the

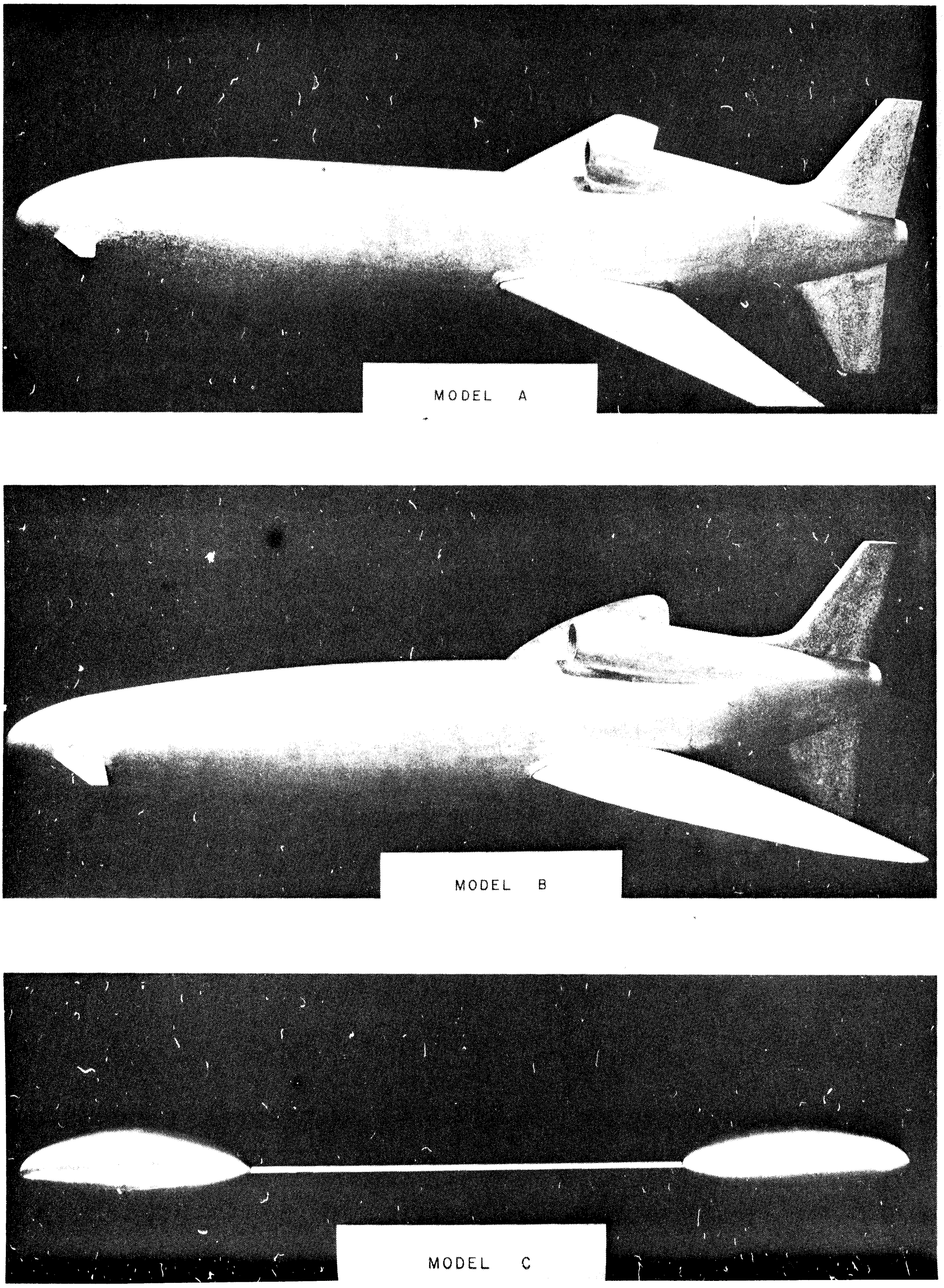

FIG. 1-1: PHOTOGRAPHS OF MODELS

wings of the aircraft for horizontal polarization (i. e. E-vector also in the plane of the wings); thus the results take the form of patterns of cross section vs θ where θ is the azimuth angle measured from nose-on in the plane of the wings.

In addition to the experimental work a theoretical study of the S-band radar cross section characteristics of Model "B" was performed together with a theoretical analysis and interpretation of the experimental data obtained.

In the following section the experimental facility and the experimental procedures employed in this study are discussed in some detail. The theoretical methods employed are as documented in Reference 1 and thus a detailed discussion of the theoretical method is not given here; a brief description of the method is given, however, in Section III.

The data obtained and the results of the theoretical analysis are presented in the concluding Section IV.

The authors whould like to acknowledge the contributions made by T. Hon and R. Wolford during the experimental portion of this study and to E. LeBaron and F. Vincent for their contributions to the theoretical-analysis phase of the program.

II. EXPERIMENTAL FACILITIES AND PROCEDURES

The measurements were made in an anechoic room 30 feet by 60 feet by 15 feet high. The absorbing material on the walls, floor and ceiling has a reflection coefficient of less than 0.01 at S-band, 0.001 at X-band and it is about 0.0001 at K-Band.

Standard equipment and techniques for CW radar scattering measurements were used. A block diagram of the equipment is given in Figure 2-1. A single horn is used for transmitting and receiving. The transmitted signal is separated from the received signal by means of a balanced hybrid tee. This technique requires a high degree of frequency stability in the oscillator. This stability was achieved at X-band by the use of a cavity stabilized oscillator and at S and K bands the frequency stability was obtained from a crystal oscillator. The receiver was of the microwave superheterodyne type using a separate mixer for each frequency band. The models were supported on a styrofoam column resting on a pedestal which could be rotated about its vertical axis. A photograph of the room and part of the equipment is given in Figure 2-2 and Figure 2-3 shows model B on the polyfoam support.

In order to have the target illuminated by a plane wave the antenna-target separation distance should be $2D^2/\lambda$ where D is the maximum dimension of the target or antenna, which ever is larger. It has been shown (References 2 and 3) both analytically and experimentally that the

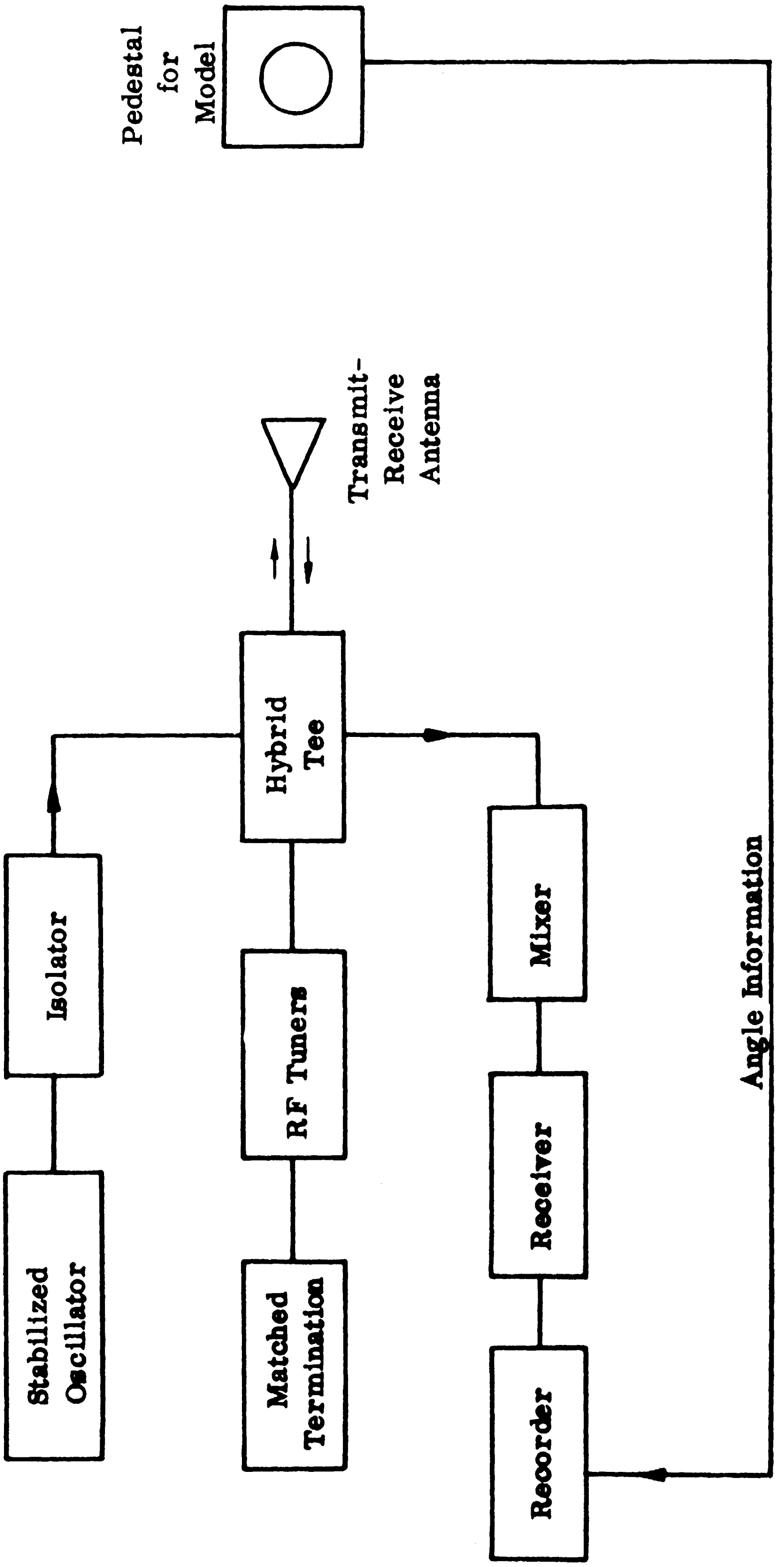

FIG. 2-1: BLOCK DIAGRAM OF EQUIPMENT

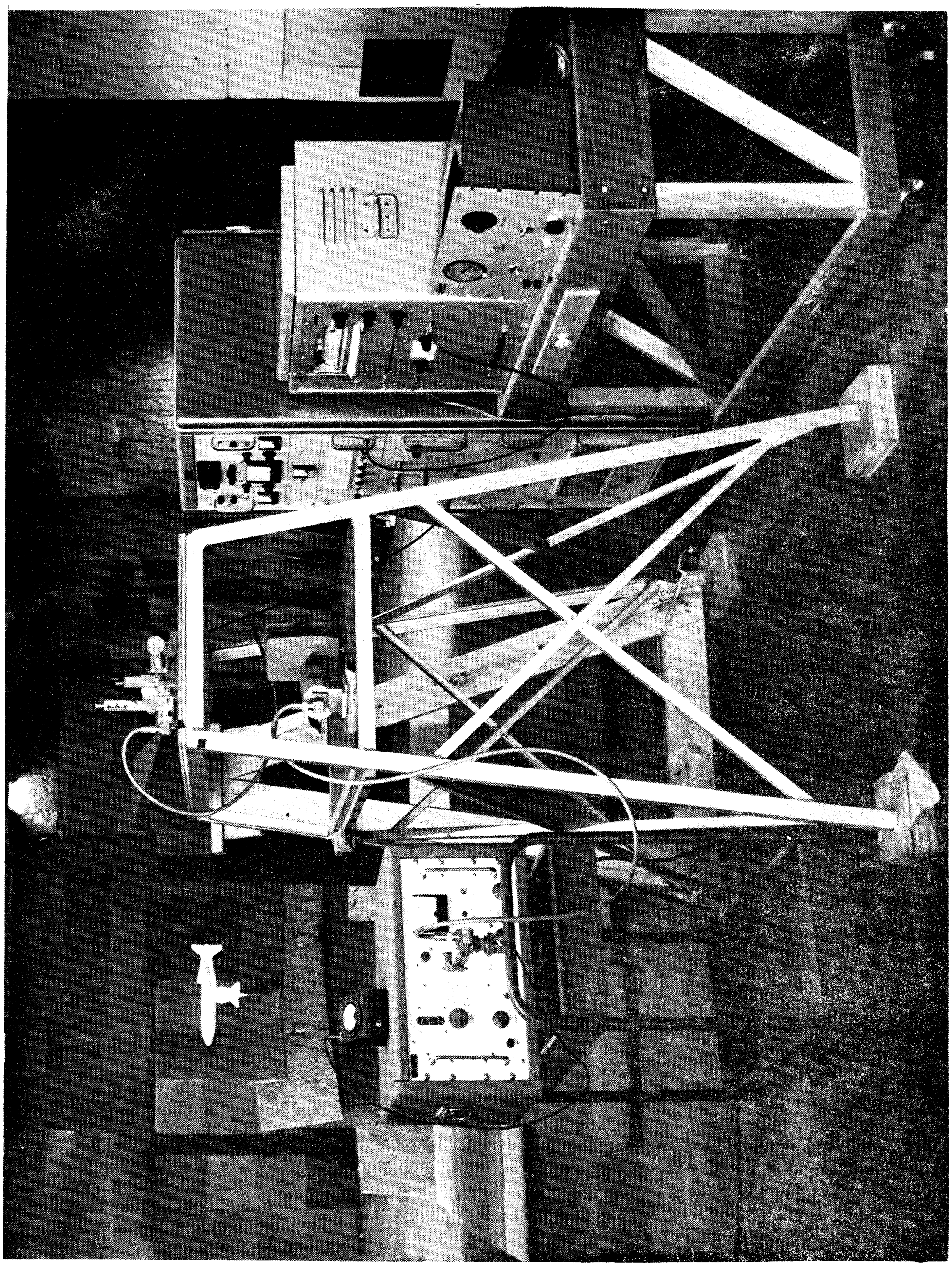

FIG. 2-2: PHOTOGRAPH OF ROOM AND EQUIPMENT

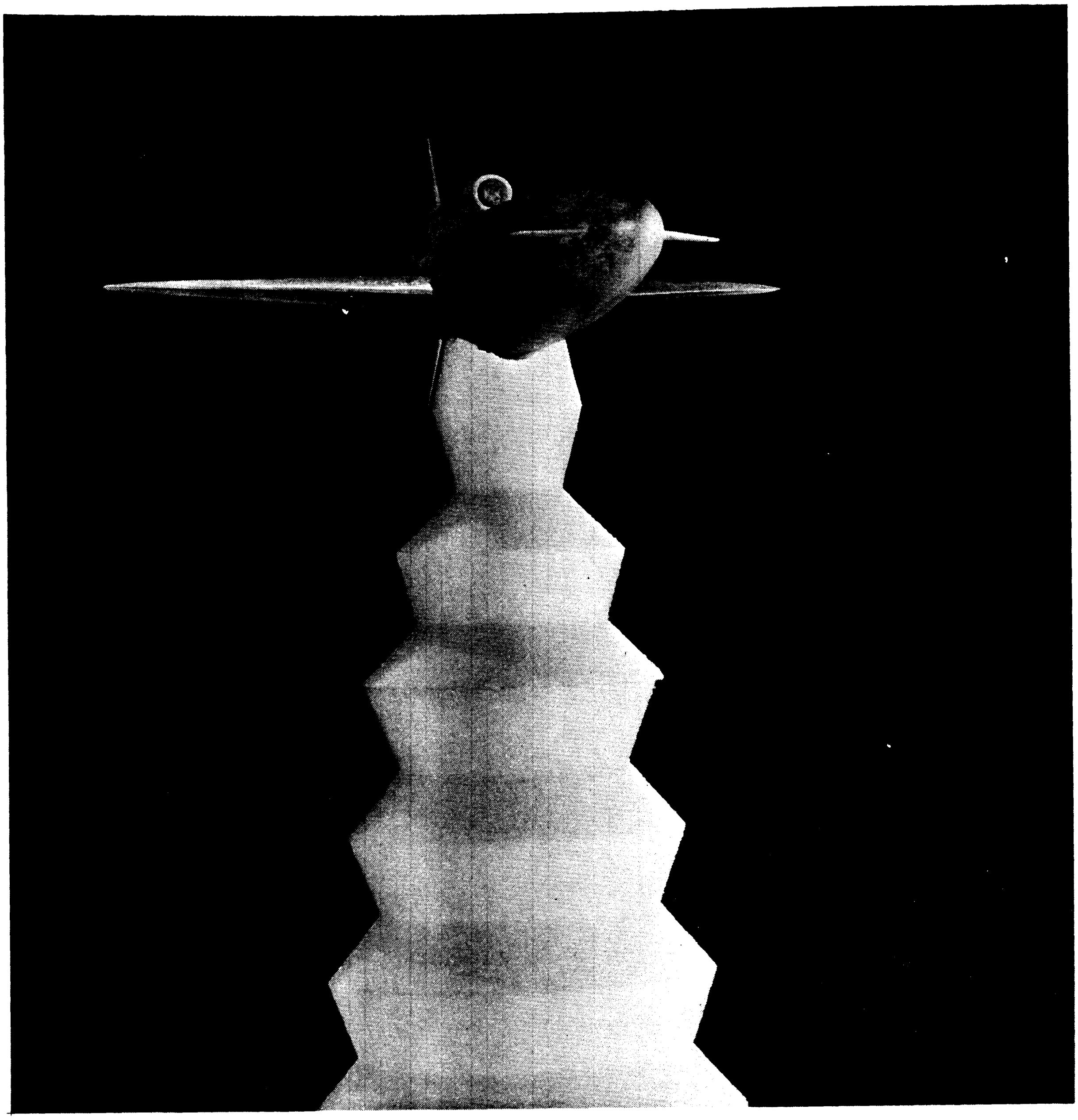

FIG. 2-3: PHOTOGRAPH OF MODEL ON POLYFOAM SUPPORT

errors involved in working at D^2/λ are too small to be significant for most application and that in general, it is possible to work much closer than D^2/λ. Studies made at Ohio State (Ref. 3) concerned the effect of range as range was decreased to as short as $D^2/13\lambda$. The results led them to the conclusion that there is little range sensitivity for round trip phase deviations of as much as 6.6π between the antenna and the target center as compared to the distance from the antenna to the target extremity, with the target in the broadside position.

The D^2/λ distances for a 32 inch target at the S, X and K-band frequencies used are 21, 70 and 165 feet respectively. The ranges used in these measurements were generally about 25 feet although some measurements were made at a range of 40 feet. For a 32 inch model at 23 kmc, the round trip phase deviation is about $1.5\ \pi$. It is believed, therefore, that no appreciable error resulted from working at the range used.

The range illumination at the target was measured over the area occupied by the target. At S-band, the decrease in power from the center to the edge of the target area was 1 db in the horizontal plane and 0.5 db in the vertical plane. At X-band, corresponding figures were 0.8 db in the horizontal and 0.5 in the vertical. These measurements were not made at K-band; as a result of the smaller K-band horn beamwidth it is expected that the decrease in power would be about 2 db and one db in the horizontal and vertical planes respectively.

The reflections from the background are balanced out or cancelled out before the target is placed on the pedestal. When the target is placed on the pedestal, new reflections from the background result from the forward scattering of the target. The effect of these are minimized by adjusting moveable absorbing panels in the background. The remaining contribution from the background will either increase or decrease the return from the target, depending on the relative phase of the two signals. By taking two or more patterns where the range was varied by $\lambda/4$, it is possible to determine the average pattern which is the true pattern from the target. This practice was followed in this series when the background contribution was significant. The patterns included in the report were chosen as representative of the average patterns of the several taken for a particular model and frequency. The effect of the background may amount to 2 or 3 db when the target is viewed nose-on but it is usually less than one db when the target is viewed at or near broadside aspects.

A standard sphere at S and X-band and a standard corner reflector at K-band was used to calibrate the model patterns in square meters. The level of the one square meter cross section area (at the simulated frequency) is shown on each pattern.

III. THEORETICAL PROCEDURES

As stated in the Introduction the theoretical methods employed in this study are documented in Reference 1. It seems warranted, however, to make a few brief comments on the method here prior to proceeding to the application of the method to the Boeing models. The theoretical method for the calculation of the radar cross section of an aircraft consists essentially of three steps:

(1) The body is considered to be an ensemble of components each of which can be geometrically approximated by a "simple" shape in such a way that the radar cross section of the simple shape approximates the radar cross section of the component it models. The first step, thus, in this theoretical method consists of a geometrical breakdown (or model construction) of the configuration.

(2) The second step involves the calculation of the cross sections of the simple shapes derived in step (1). This requires the application of various approximation methods in most cases since "exact" solutions are available only for a very few simple shapes.

(3) The third and final step in this process involves the proper combination of the "component cross sections" to yield the estimate of the cross section of the entire body.

In the event that one is interested in determining the trends in the radar cross section variation with aspect or frequency the approach for step (3) is one in which the relative phases between the various contributions are averaged out. This results in the "random phase" or "average" radar cross section pattern which has been found to yield results agreeing with experimental data to within 6 db over most ranges of frequency and aspect.

The application of step (1) is illustrated in Appendix A where the theoretical analysis of model B is discussed; an example of the type of agreement between theory and experiment obtained is also illustrated there.

IV. RESULTS OF STUDY

4.1 The Experimental Data

Ten patterns of radar cross section vs. aspect were obtained. They include the patterns for Models "A", "B", and "C" at each of the model frequencies of 22,960; 9800; and 2870 mcs. The patterns are reproduced in Figures 4.1-1 through 4.1-10 as listed in Table I. Discussions of the data

Table 1

Pattern No.	Model	Model Frequency (mcs)	Simulated Frequency (mcs)
1	A	2870	287
2	B	2870	287
3	C	2870	287
4	A	9800	980
5	B	9800	980
6	B*	9800	980
7	C	9800	980
8	A	22,960	2296
9	B	22,960	2296
10	C	22,960	2296

*The vertical fins of model B are covered with a -20 db radar absorbing material.

are contained in Section 4.2. It is believed that the lack of symmetry in some parts of the patterns is due largely to a lack of symmetry in the models, particularly in the wings. The asymmetries are also due, in part, to a lack of symmetry in the room.

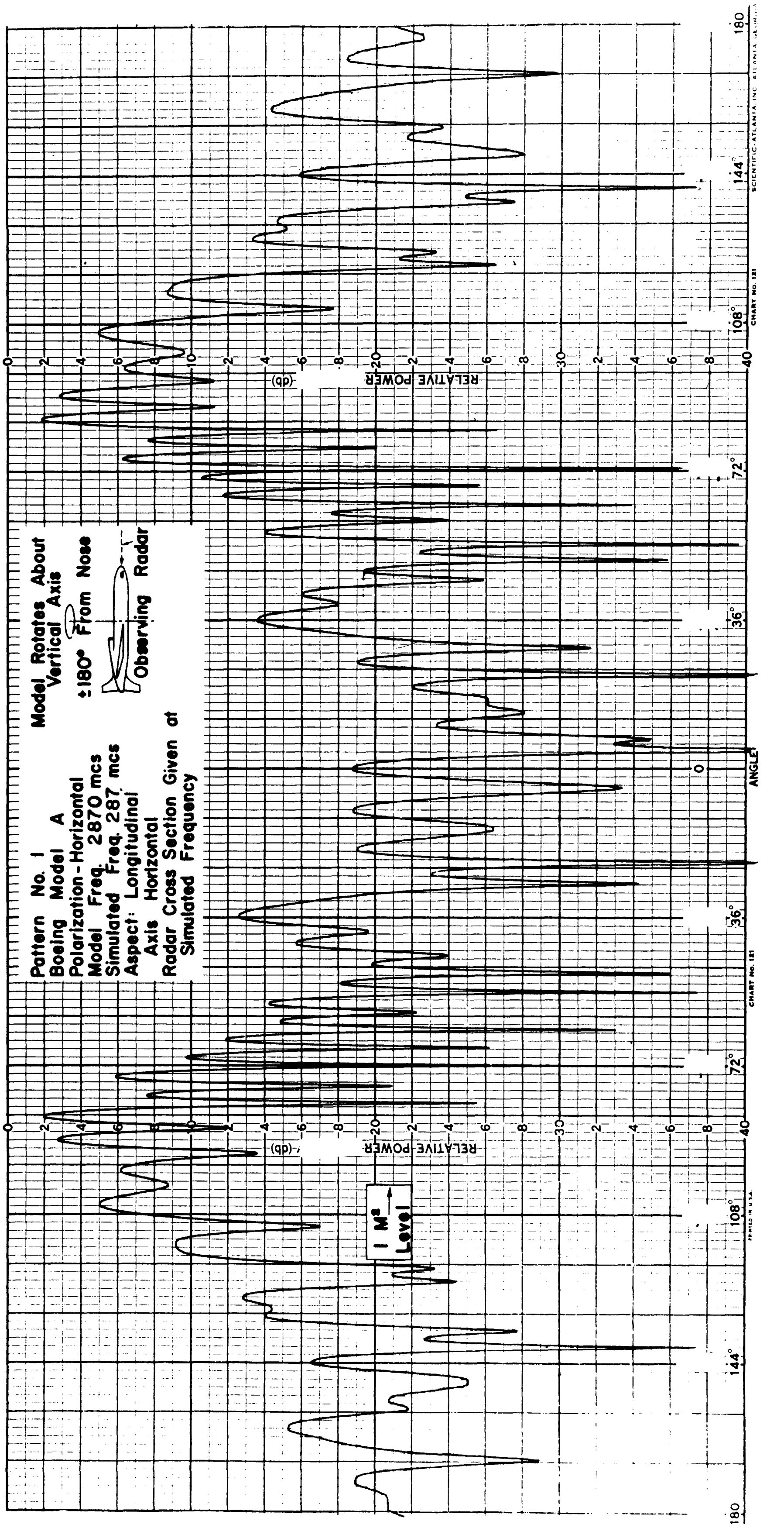

FIG. 4.1-1: PATTERN No. 1

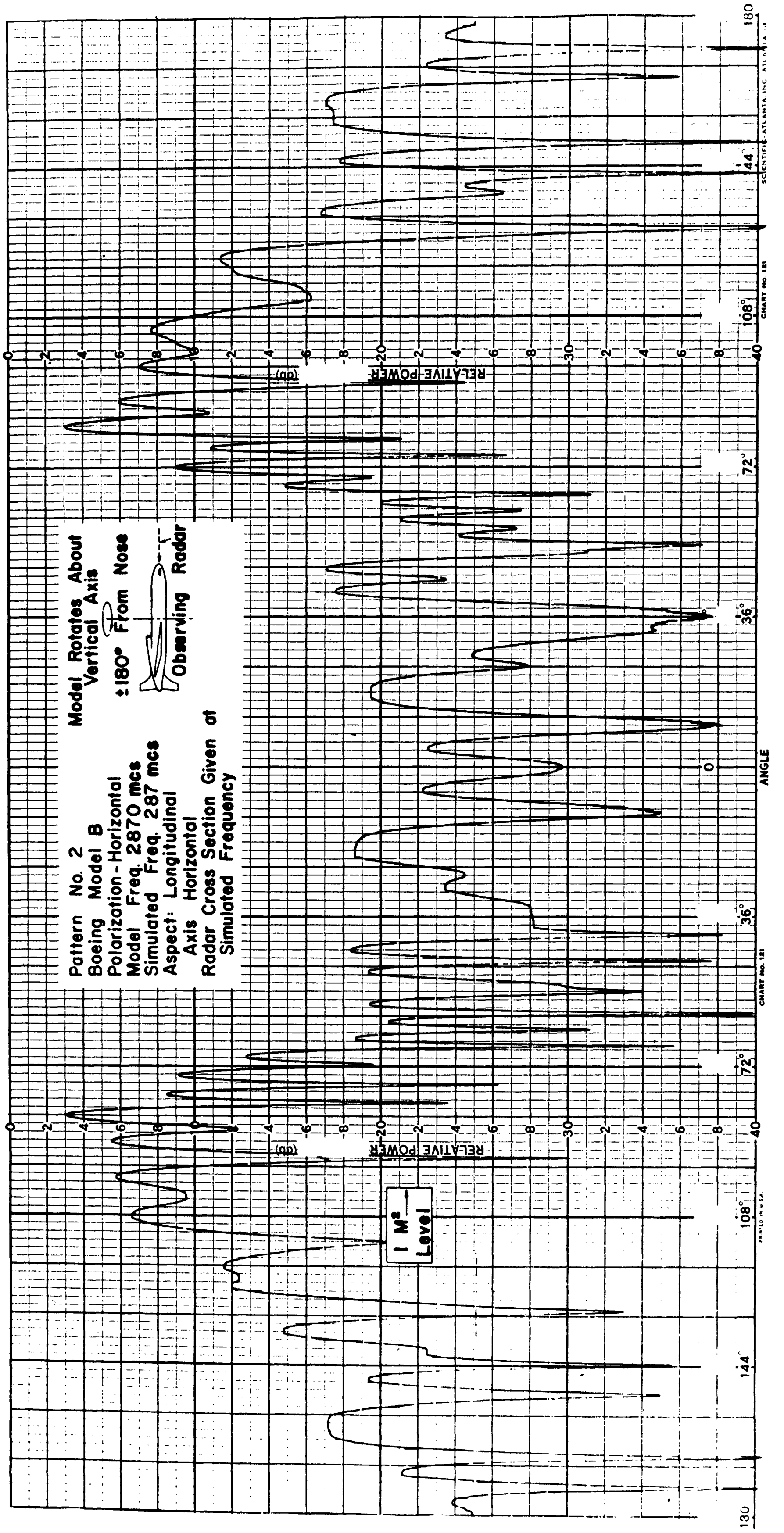

FIG. 4.1-2: PATTERN No. 2

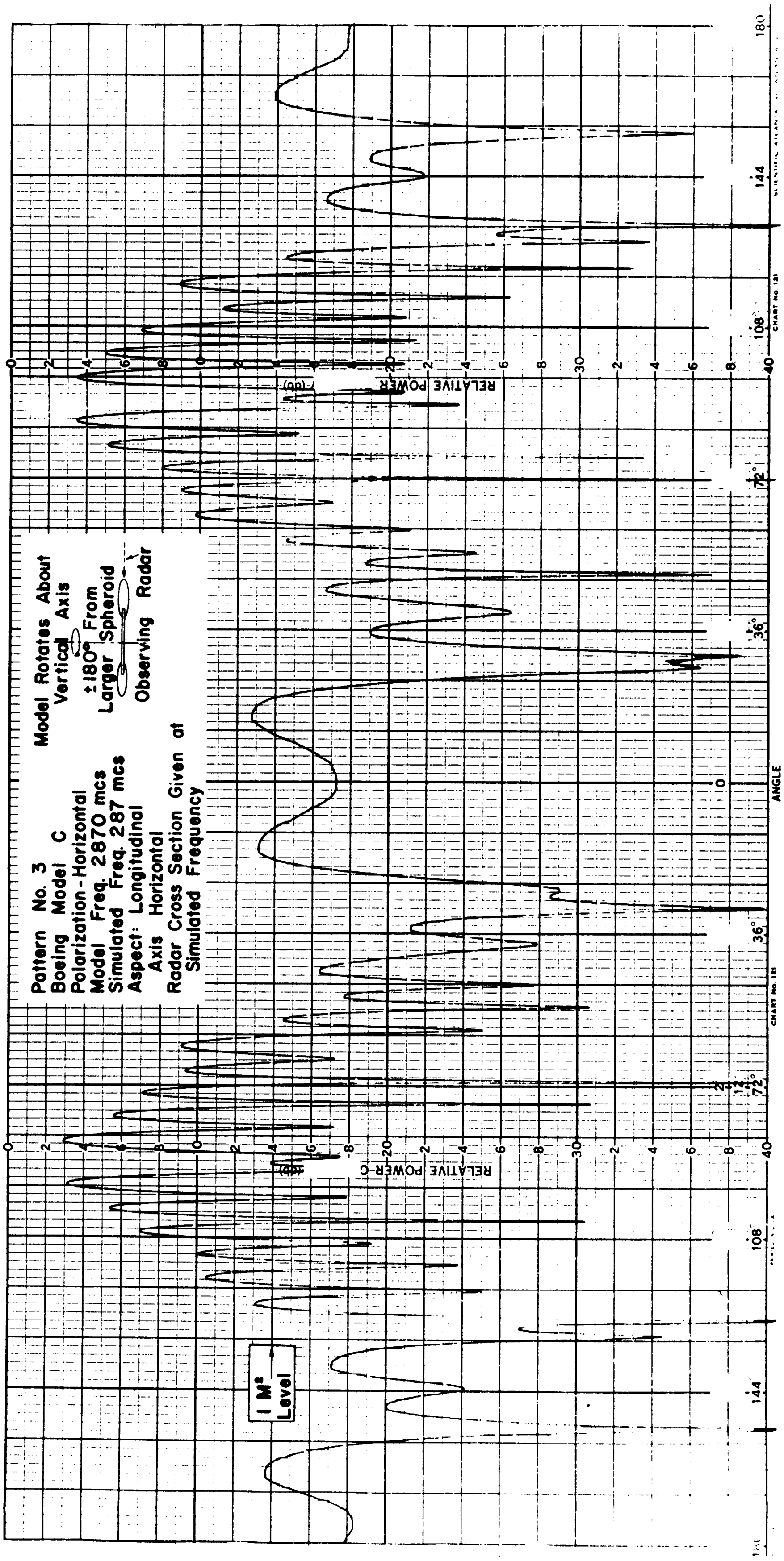

FIG. 4.1-3: PATTERN No. 3

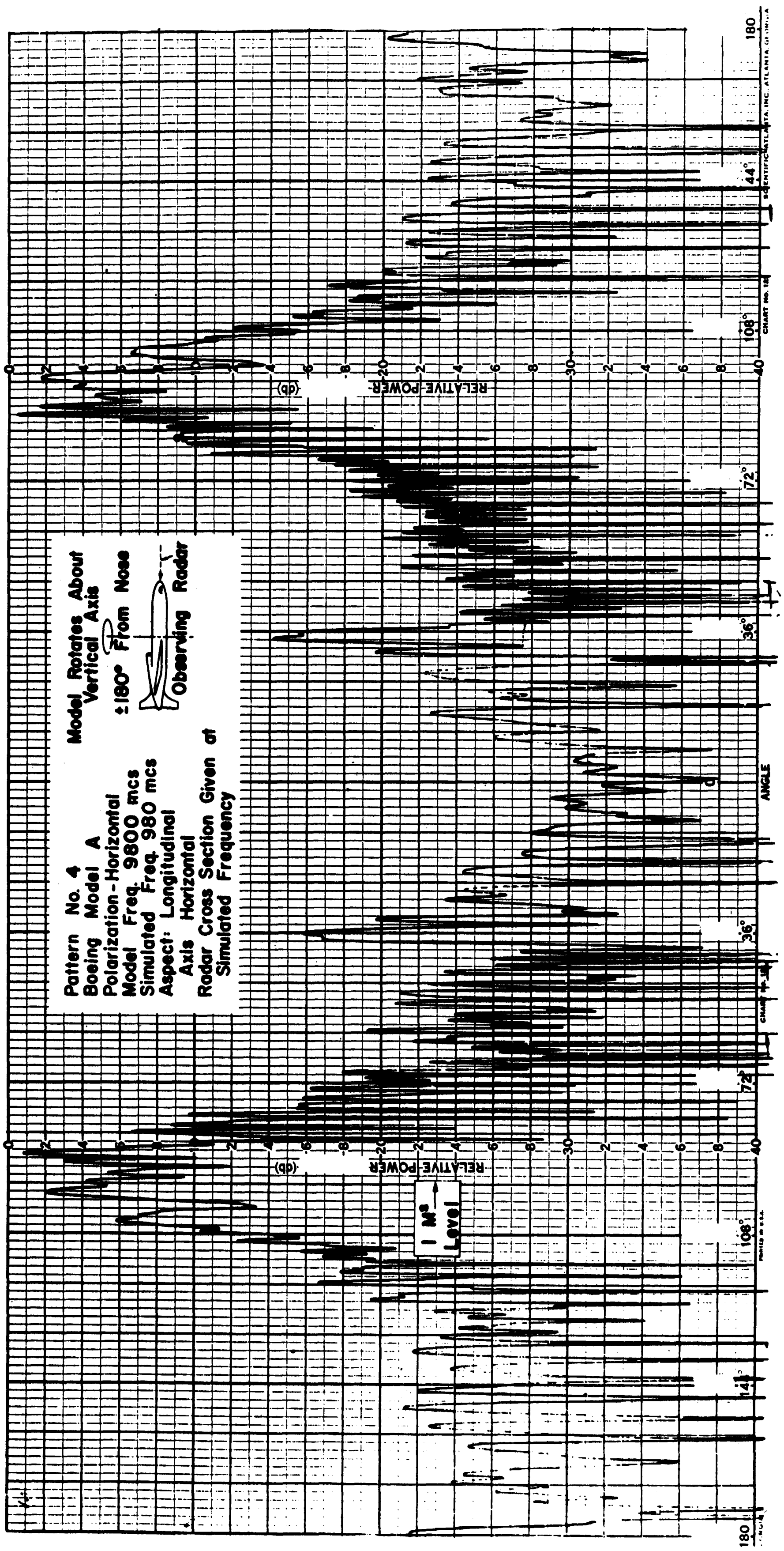

FIG. 4.1-4: PATTERN No. 4

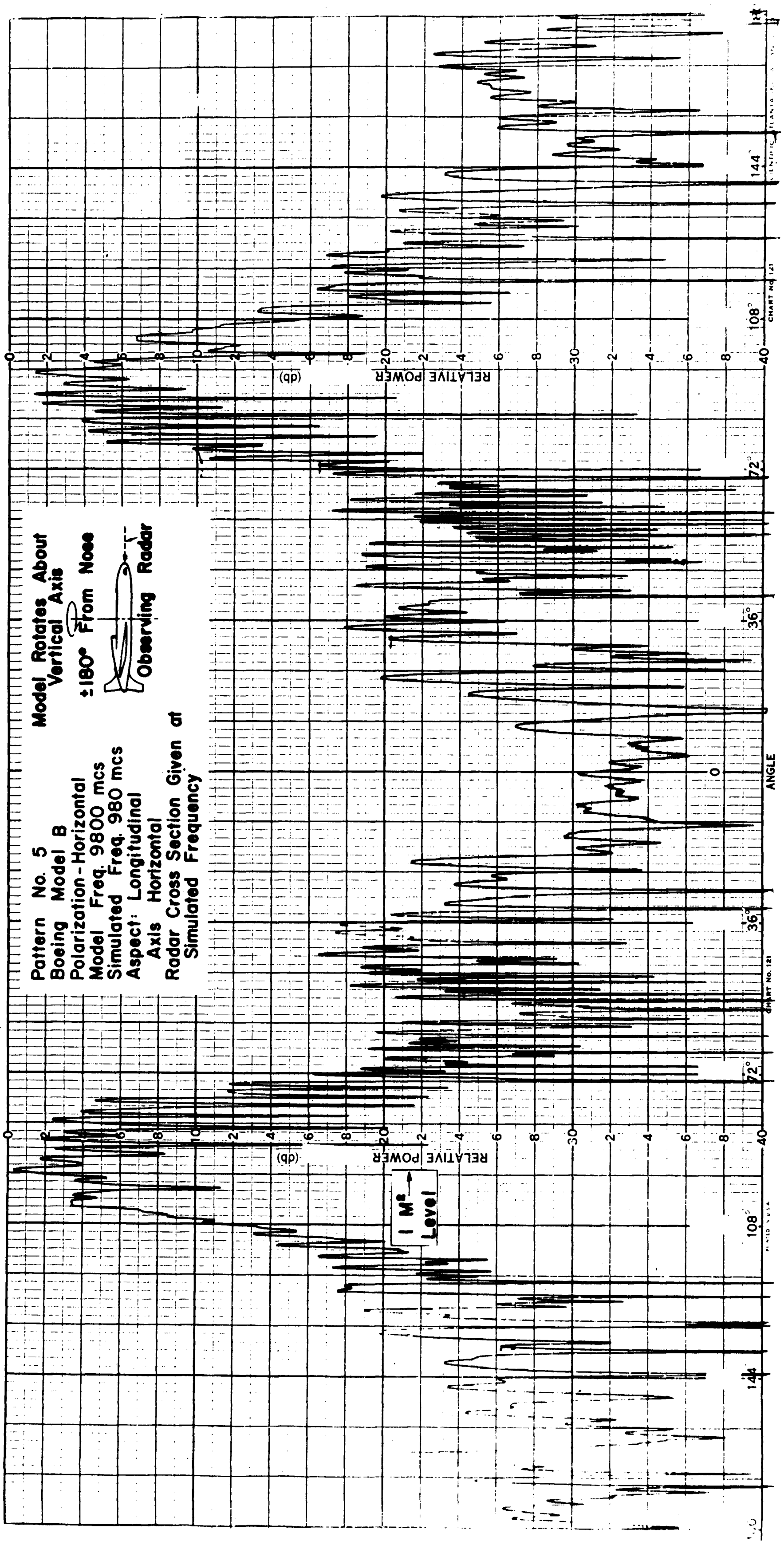

FIG. 4.1-5: PATTERN No. 5

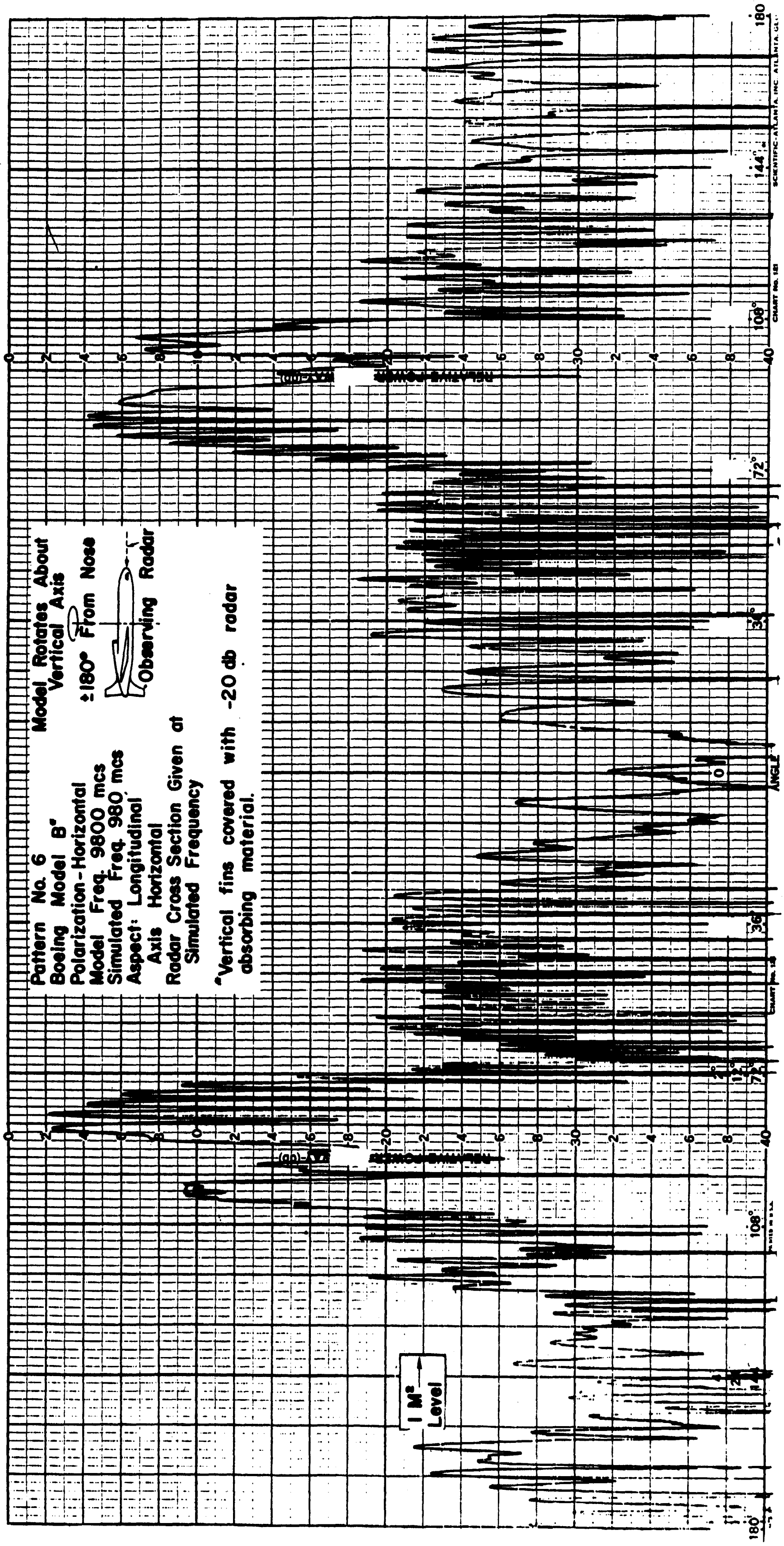

FIG. 4.1-6: PATTERN No. 6

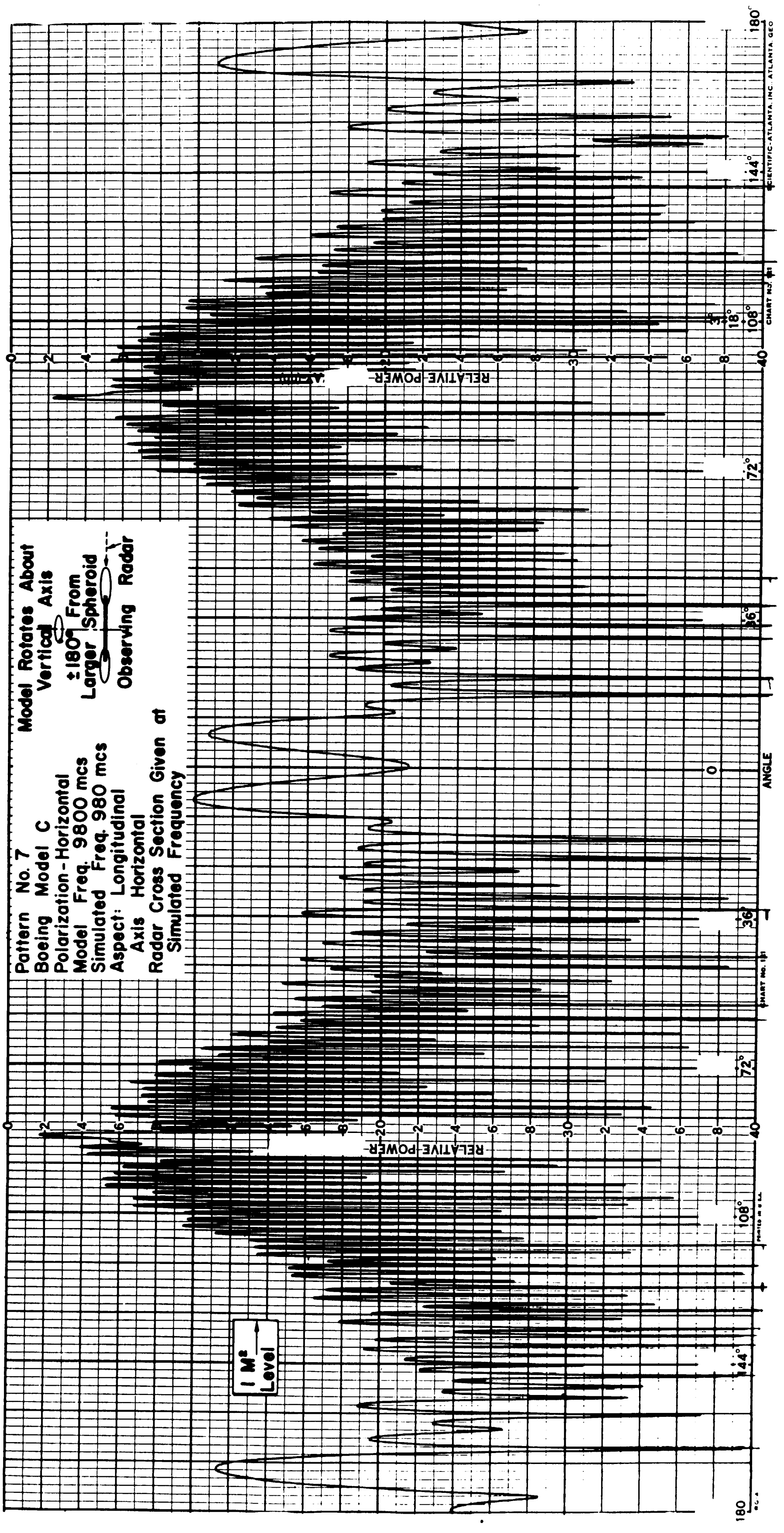

FIG. 4.1-7: PATTERN No. 7

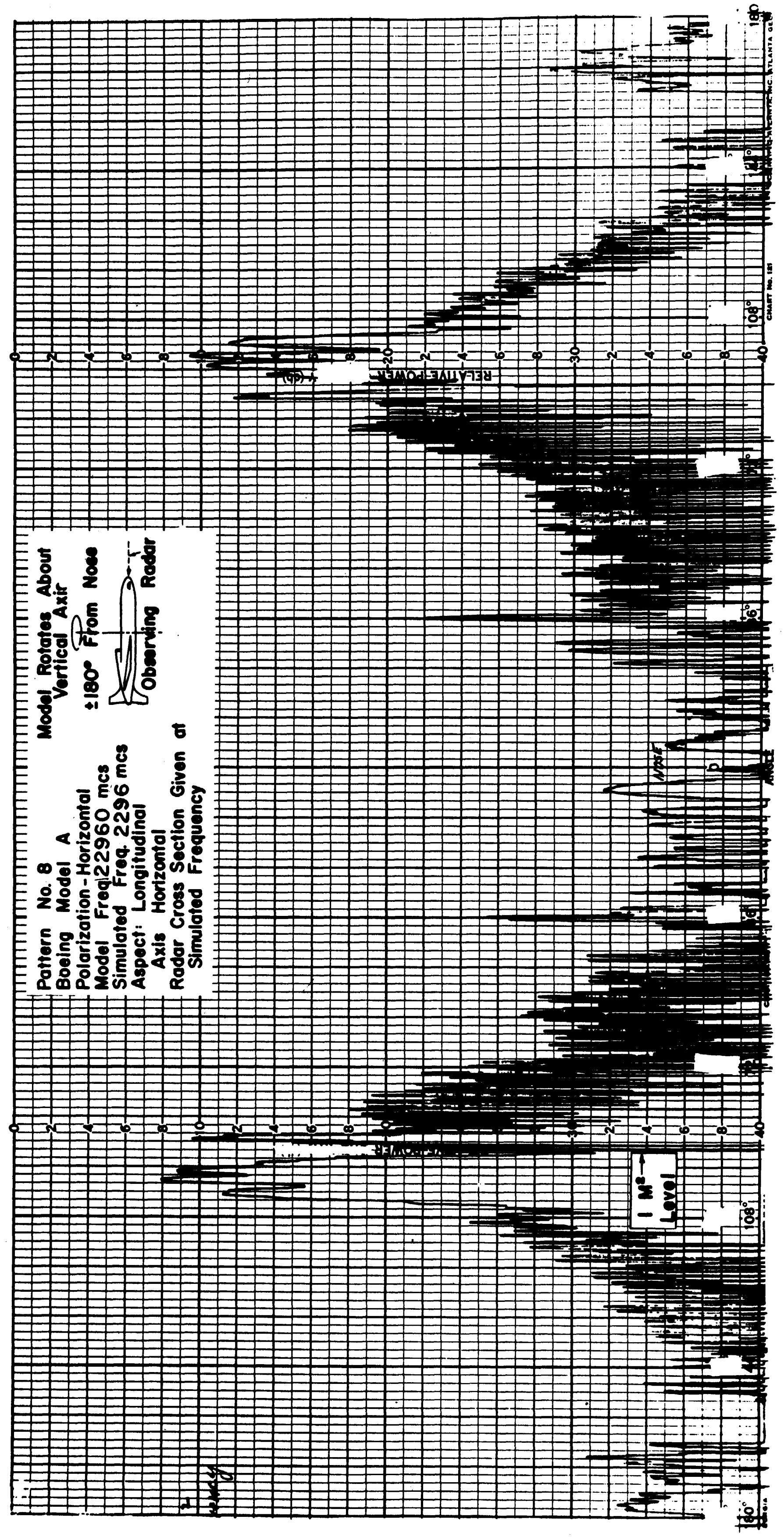

FIG. 4.1-8: PATTERN No. 8

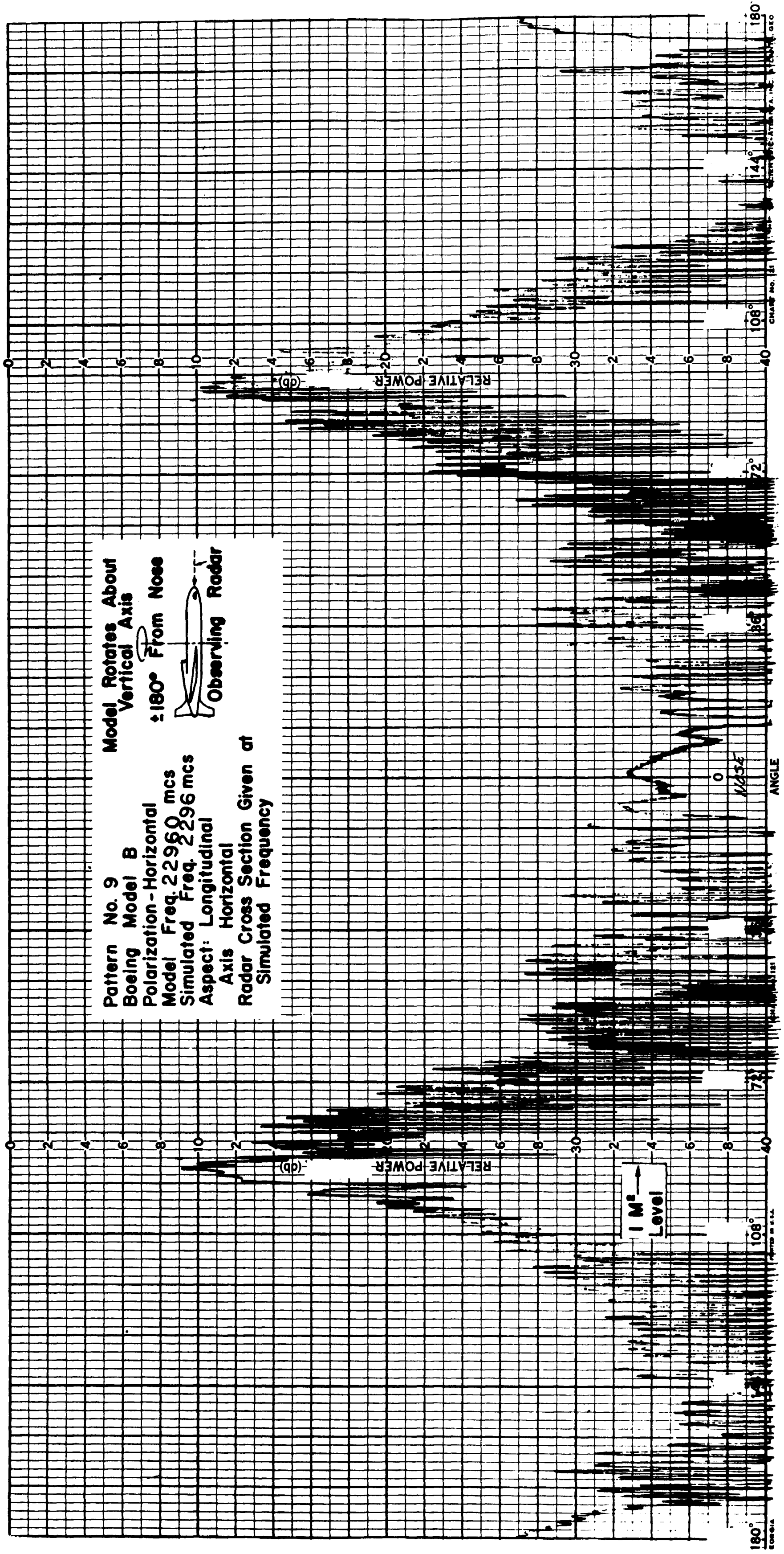

FIG. 4.1-9: PATTERN No. 9

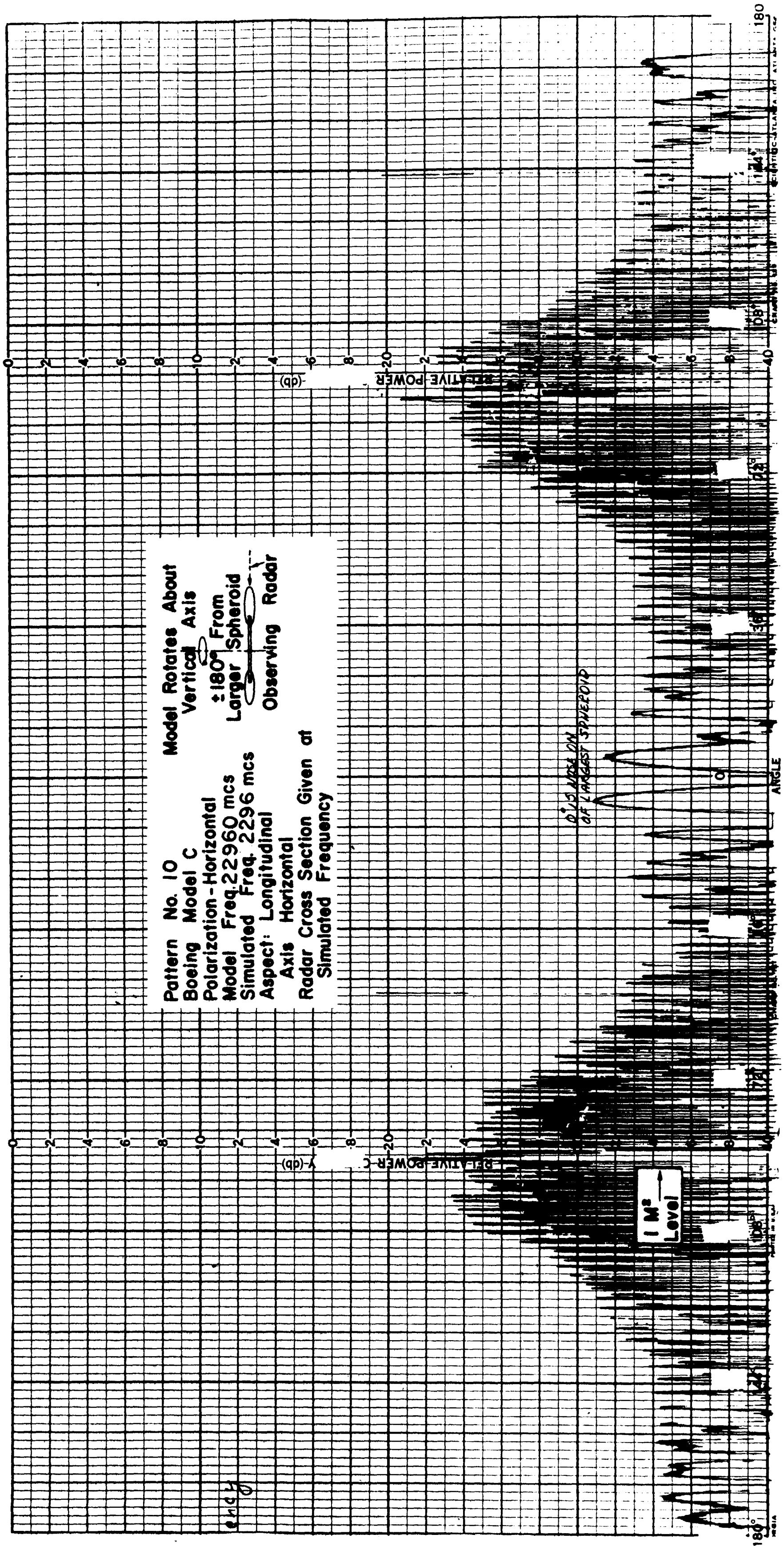

FIG. 4.1-10: PATTERN No. 10

An additional study was performed relative to Model "B" at 9800 mcs to determine the role played by the vertical fin. This pattern is reproduced in Figure 4.1-6. The modification consisted of covering the vertical fin with a good absorbing material and it will be observed (by comparing Figures 4.1-5 and 4.1-6) that in the aspect interval $72^{o} < \theta < 90^{o}$ the elimination of the vertical fin contribution through the use of the absorbing material has little effect. However, in the interval $90^{o} < \theta < 108^{o}$ we note that the maximum value of σ in the "absorber-on-fin" case is from 5 to 9 db below the relative peaks for the "bare-fin" case.

4.2 Theoretical Analysis

4.2.1. Model "A"

A theoretical investigation of the radar cross section characteristics of Model "A" was not performed; theoretical analyses of a detailed nature were reserved for Model "B" at S-band. However, a brief analytical study of the experimental data was performed. To do this maximum and median values over 12^{o} intervals were determined from the patterns shown in Section 4.1 with the intervals centered at $\theta = 0^{o}, 12^{o}, 24^{o}, \ldots, 168^{o}$ and 180^{o}. The resulting "maximum-curves" for Model "A" are shown in Figure 4.2-1 and the resulting "median-curves" are displayed in Figure 4.2-2. The maximum-curves were obtained here at the University of Michigan while the

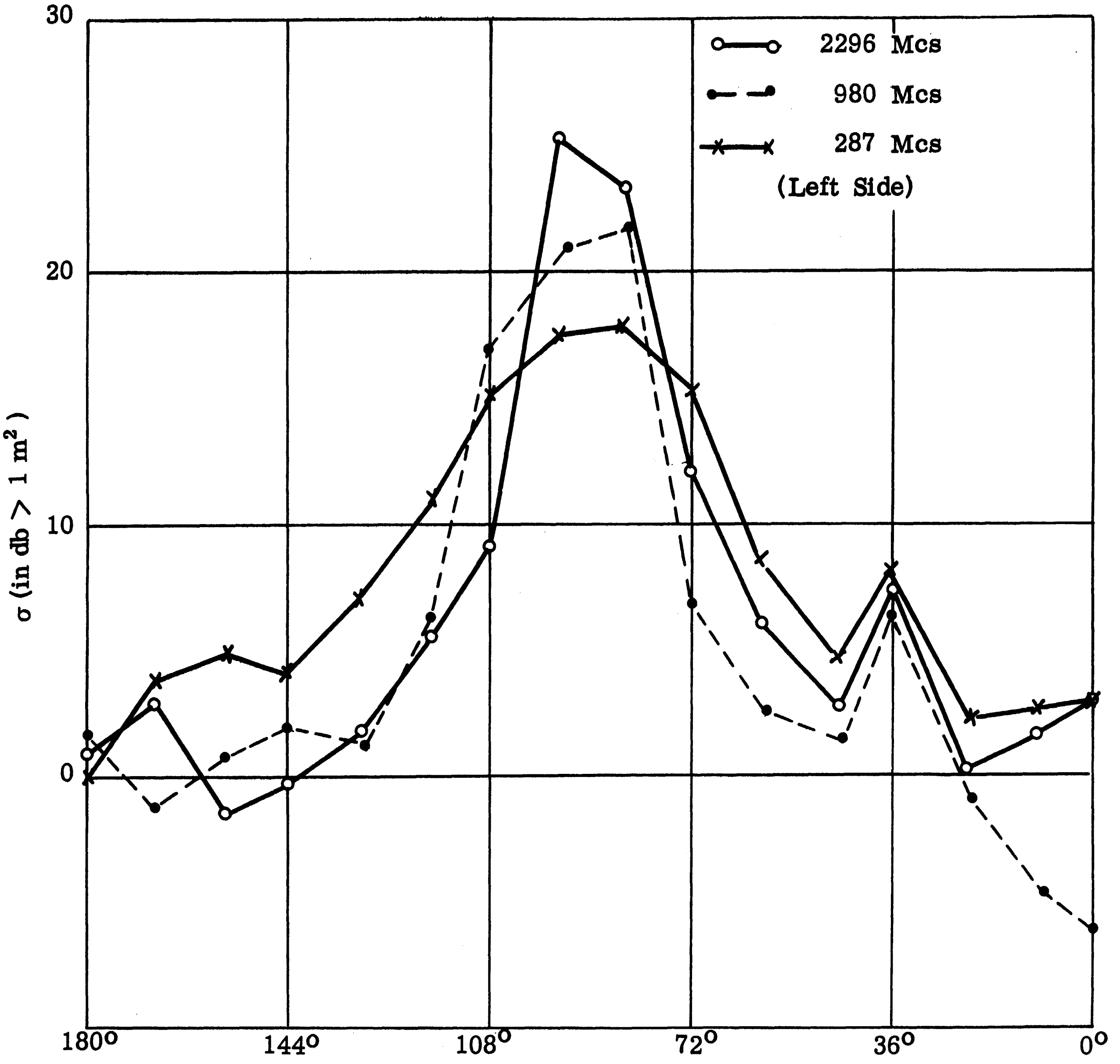

FIG. 4.2-1: RADAR CROSS SECTION OF MODEL "A" AS A FUNCTION OF ASPECT AND FREQUENCY - FULL SCALE - MAXIMUM VALUES OVER 12° INTERVALS

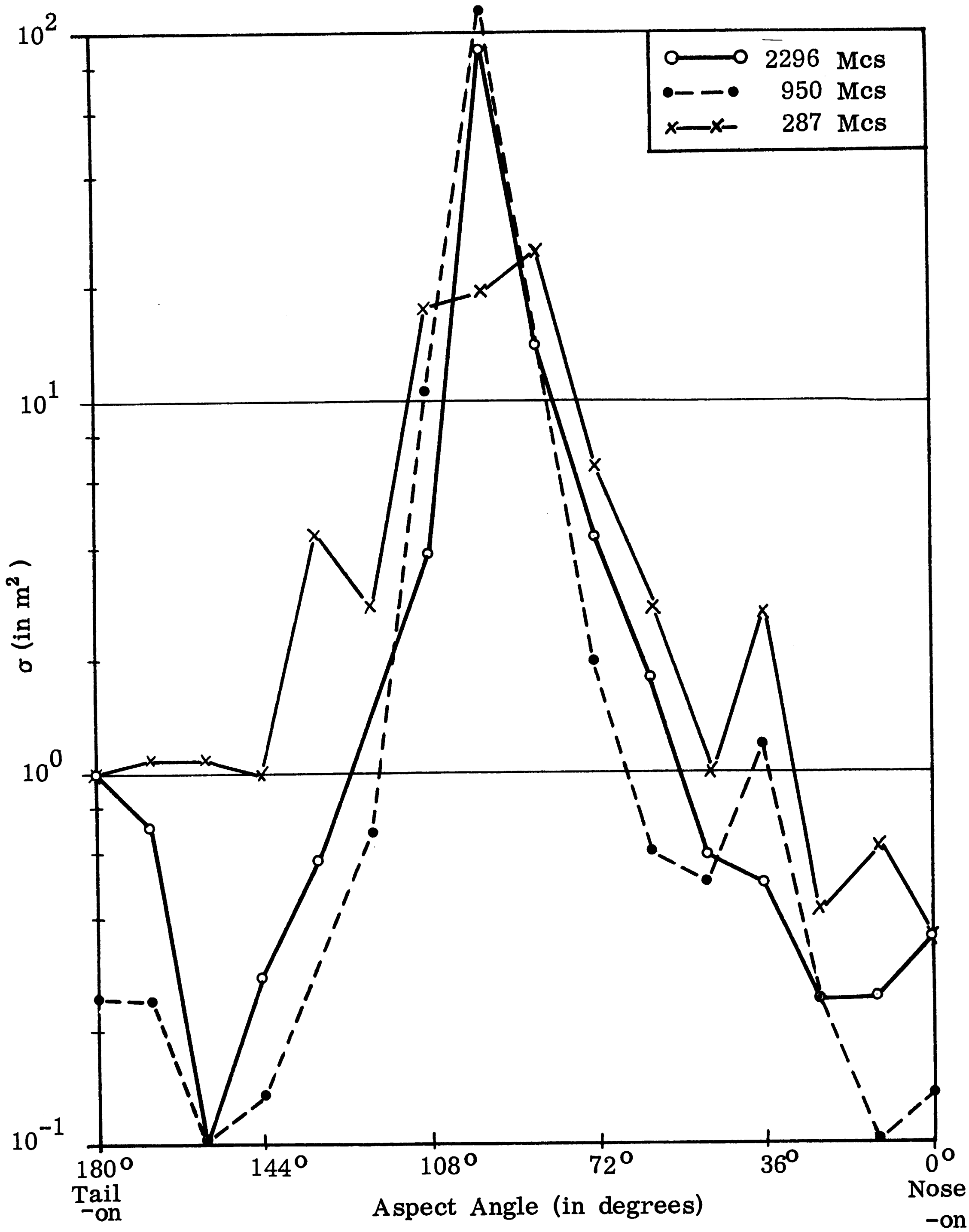

FIG. 4.2-2: RADAR CROSS SECTION OF MODEL "A" AS A FUNCTION OF ASPECT AND FREQUENCY - FULL SCALE - MEDIAN VALUES OVER 12° INTERVALS

median-curves were derived by Boeing Airplane Company personnel from copies of the patterns sent to them by the University, except that the 950 mcs data shown in Figure 4.2-2 was derived from experimental data obtained in Seattle. (Comparison of this curve with the University's 980 mcs pattern indicates that it is a reasonably good fit to the median-curve at 980 mcs also.)

Examination of Figures 4.2-1 and 4.2-2 show that the data near broadside exhibits the $1/\lambda$-type dependence expected for the cross section of this aircraft. From Figure 4.2-1 we see that in the interval from 90^{o} to 102^{o} the peak value at 2296 mcs is about 5 db above the peak value at 980 mcs (theory would imply a 4 db ratio) and the peak at 2296 mcs is about 8 db above the peak value at 287 mcs (theory would imply a 9 db ratio).

Also, for the off-broadside aspects, the theoretical approach would imply that at most aspects (the notable possible exceptions being nose-on, tail-on, and normal to the leading edge of the wing) the cross section would be, on the average, independent of frequency especially in the 980-2296 mcs range. The beginning of some resonant effects could be expected at frequencies in the 300 mcs range. These characteristics are exhibited in Figures 4.2-1 and 4.2-2.

The presentation of the 12^{o}-median curves brings up a point of interpretation which warrants discussion here. If the pattern of σ vs θ is such that there are several oscillations within a given interval (12^{o} in this case) then this "median-over-the-interval" approach does give a reasonably good representation of the "average" cross section. If on the other hand, these relative peaks are fairly well separated in such a way that only one peak occurs in a 12^{o} interval, then this approach does not always yield a "good" representation of the average curve.

4.2.2 Model "B"

A detailed study of the S-band radar cross section characteristics of Model B was performed; the details of that study are reported in Appendix A. Here we shall consider the analysis of the experimental data in a manner like that used in Section 4.2.1 for the model "A" data and only briefly summarize the results of the 3000 mcs theoretical study.

Maxima and median curves were obtained in exactly the same manner as in the discussion of the preceding section. (The resulting curves are shown in Figures 4.2-3 and 4.2-4) Again we observe the $1/\lambda$-type variations in σ at broadside where from Figure 4.2-3 we observe that the peak values in the 90^{o} to 102^{o} intervals obtained experimentally indicate a 5 db difference between the 980 and 2296 mcs data and a 9 db difference between the 287 and 2296 mcs data. These are the values predicted by theory to with 1 db, since theory would anticipate differences of 4 and 9 db respectively.

With regard to the off-broadside aspects, we again observe that for the most part the 2296 and 980 mcs patterns are very similar (the notable exceptions being nose-on and tail-on) while a tendency for the beginning of resonance effects is noted at 287.

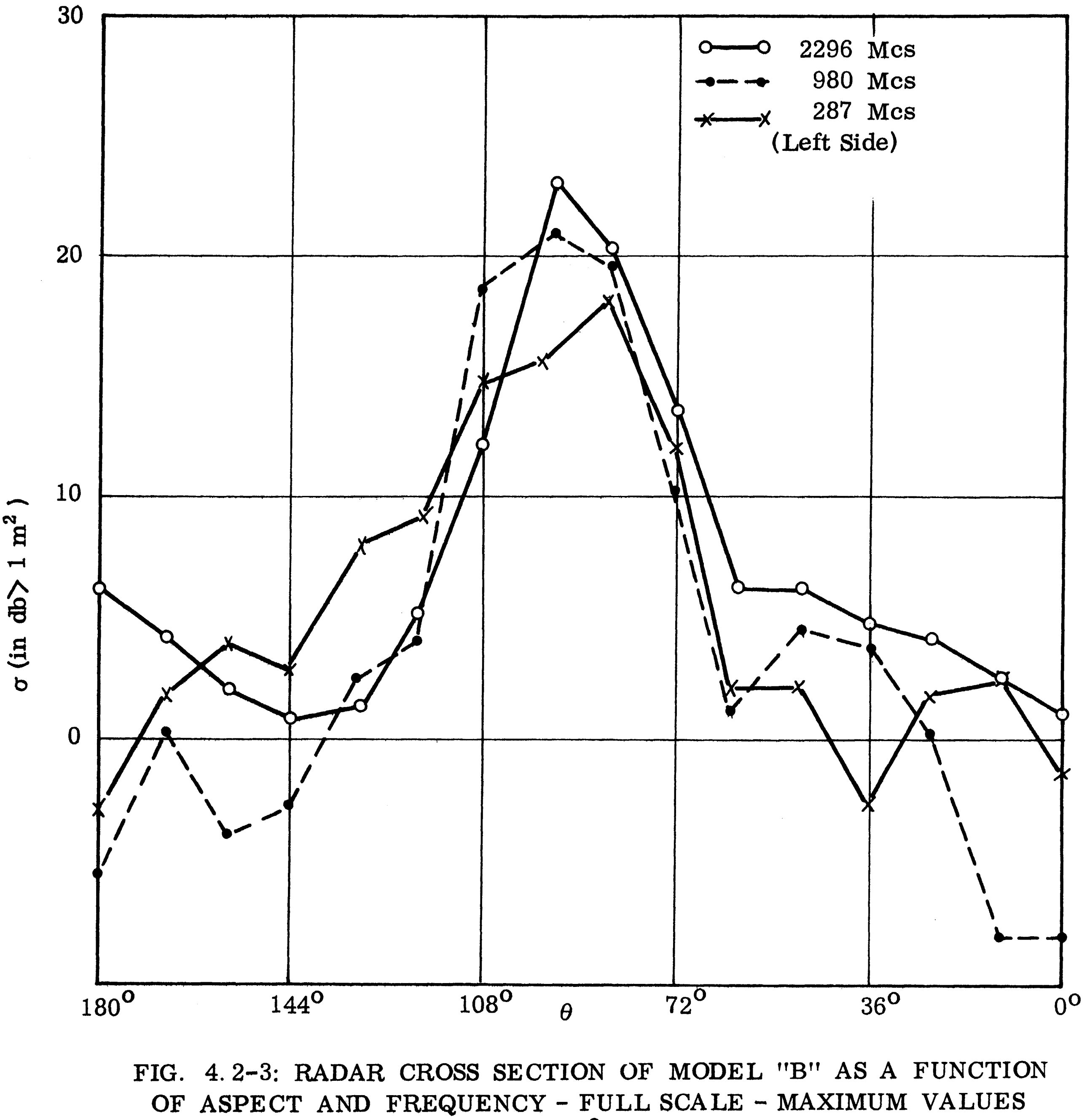

FIG. 4.2-3: RADAR CROSS SECTION OF MODEL "B" AS A FUNCTION OF ASPECT AND FREQUENCY - FULL SCALE - MAXIMUM VALUES OVER 12° INTERVALS

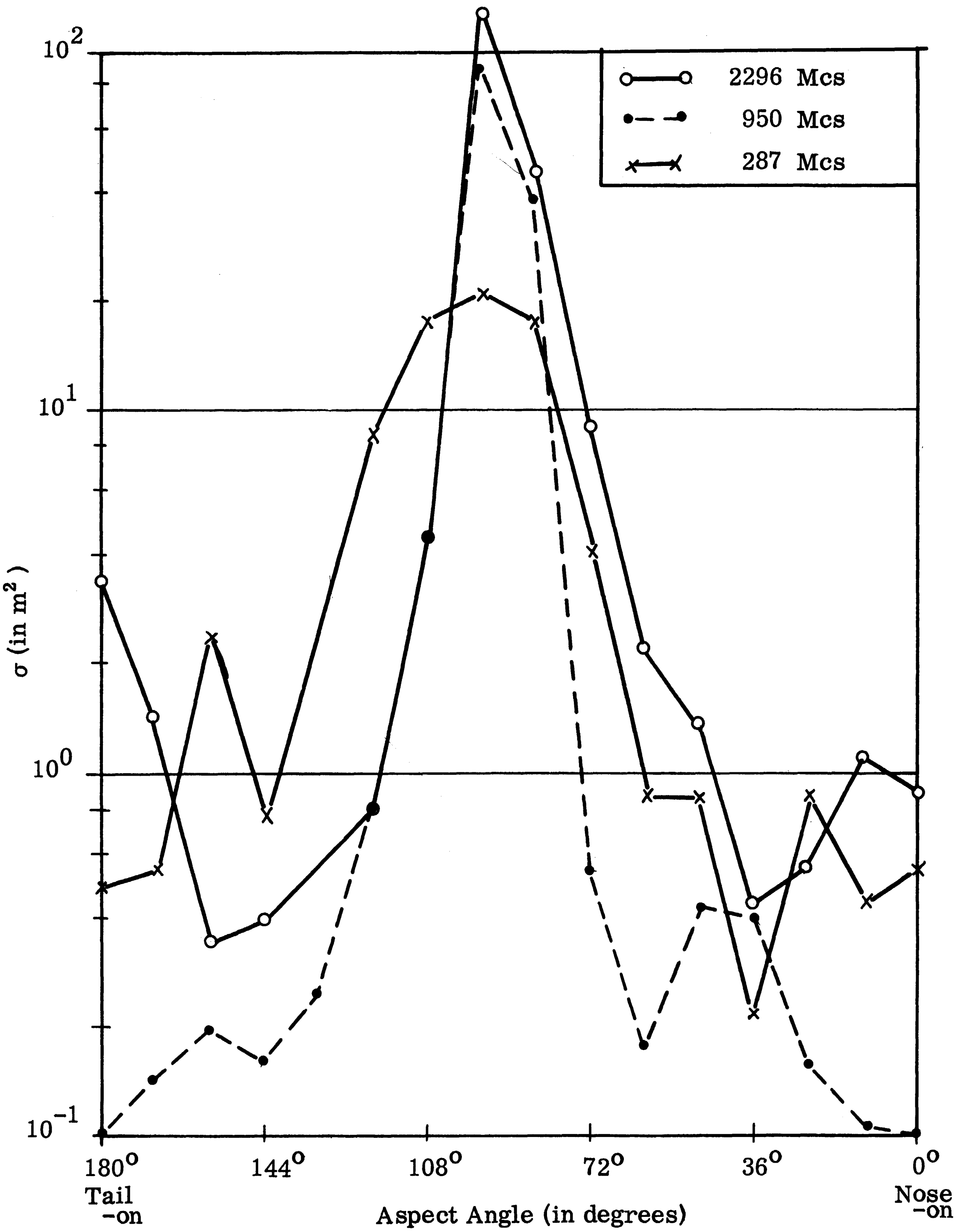

FIG. 4.2-4: RADAR CROSS SECTION OF MODEL "B" AS A FUNCTION OF ASPECT AND FREQUENCY - FULL SCALE - MEDIAN VALUES OVER 12° INTERVALS

As mentioned above the 3000 mcs theoretical study is discussed in Appendix A where the theoretical "random-phase" estimate is compared with the experimental pattern itself. Here we shall compare the theoretical "random phase" estimate with the "maximum" and "median" curves of Figures 4.2-3 and 4.2-4 at 2296 mcs (as noted in the Appendix we expect the "average" patterns at 3000 mcs and 2296 mcs to be very similar.). This comparison is made in Figure 4.2-5 we first note that the maxima and minimum curves bound the theoretical estimate everywhere except for a small region around $\theta = 156^o$, a very narrow region in the vicinity of $\theta = 12^o$, and near $\theta = 0^o$. We also observe that the 12^o-median curve does not differ from the "random phase" one by more than 5 db anywhere except in these intervals and by no more than 10 db at any of the aspects considered. A possible explanation for the differences in these three θ intervals, is that the interiors of the two cavities in the model were not as evenly covered with a conducting surface (paint) as was the exterior; an assumption which was made in the theoretical analysis.

4.2.3 Model "C"

The model "C" patterns were not studied in the same detail as were those for Models "A" and "B" but it will be of some interest to examine the frequency variation observed and the magnitudes of cross section obtained

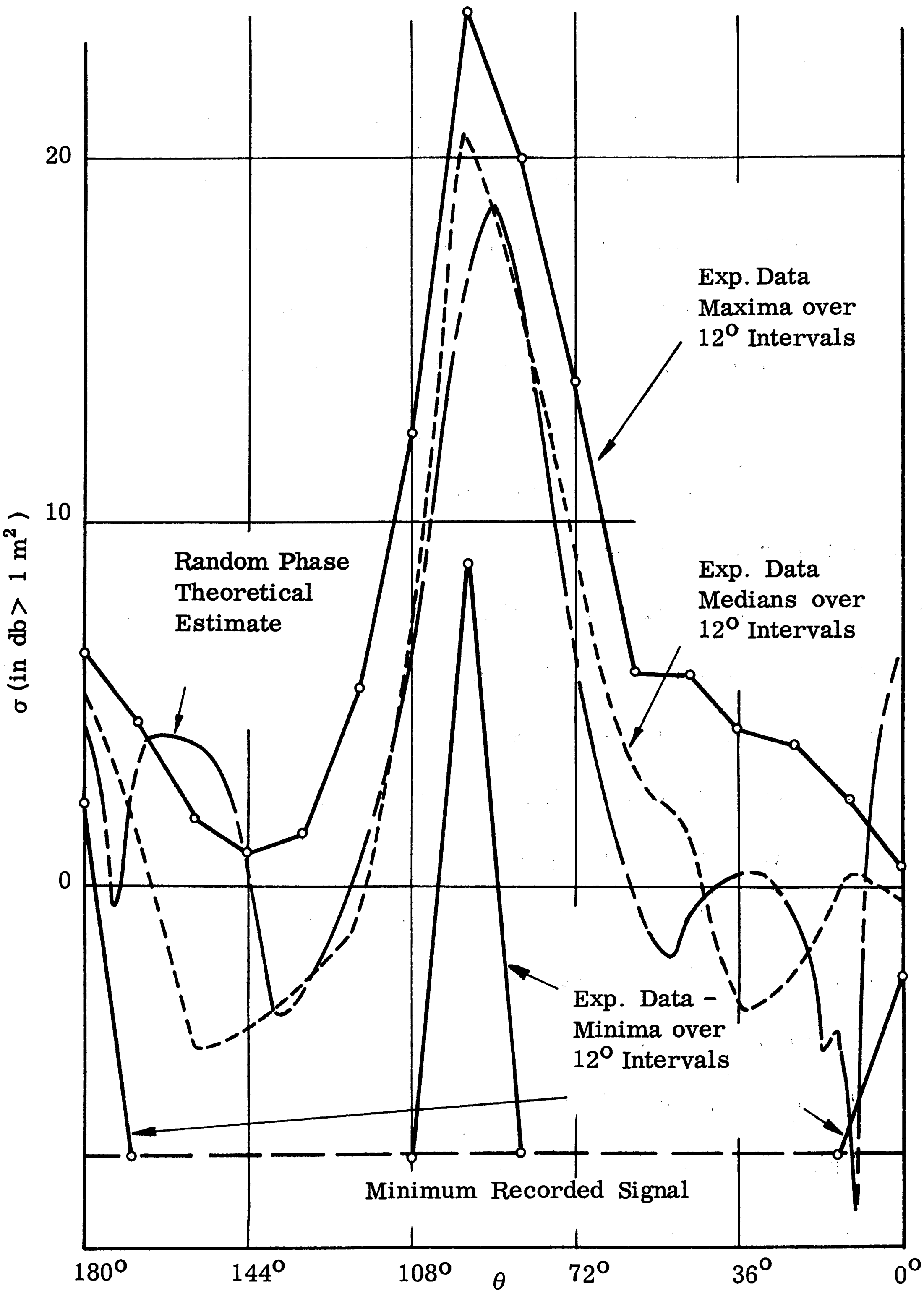

FIG. 4.2-5: MODEL "B" - A COMPARISON BETWEEN THEORY AT 3000 Mcs AND EXPERIMENT AT 2296 Mcs

in the light of the theoretical method. In Figure 4.2-6 we present a rough sketch of Model "C" with the model dimensions indicated (the dimensions given are approximate having been measured from the model itself; they are sufficiently accurate for our purposes here" and in Figure 4.2-7 we display the "maximum-over-12°-interval" curves obtained from the patterns obtained at the "full-scale" frequencies of 980 and 2296 mcs.

By the theoretical method we would conclude that the cross section for all aspects in the range from $\theta \approx 30^\circ$ to $\theta \approx 150^\circ$ would be largely governed at these frequencies by the optics response from the two spheroids with the cylinder contributing appreciably only at $\theta = 90^\circ$. For the case of θ near nose-on or near tail-on in this horizontal polarization case the theoretical studies of cross sections of long thin bodies would anticipate a resonant type peak a few degrees off the axis. (This point is discussed on page 264 of Reference 1.) This approach would imply that relative peaks in σ should be observed at

(a) θ slightly less than 11° at 980 mcs

(b) θ slightly more than 169° at 980 mcs

(c) θ slightly less than 7° at 2296 mcs

(d) θ slightly more than 173° at 2296 mcs

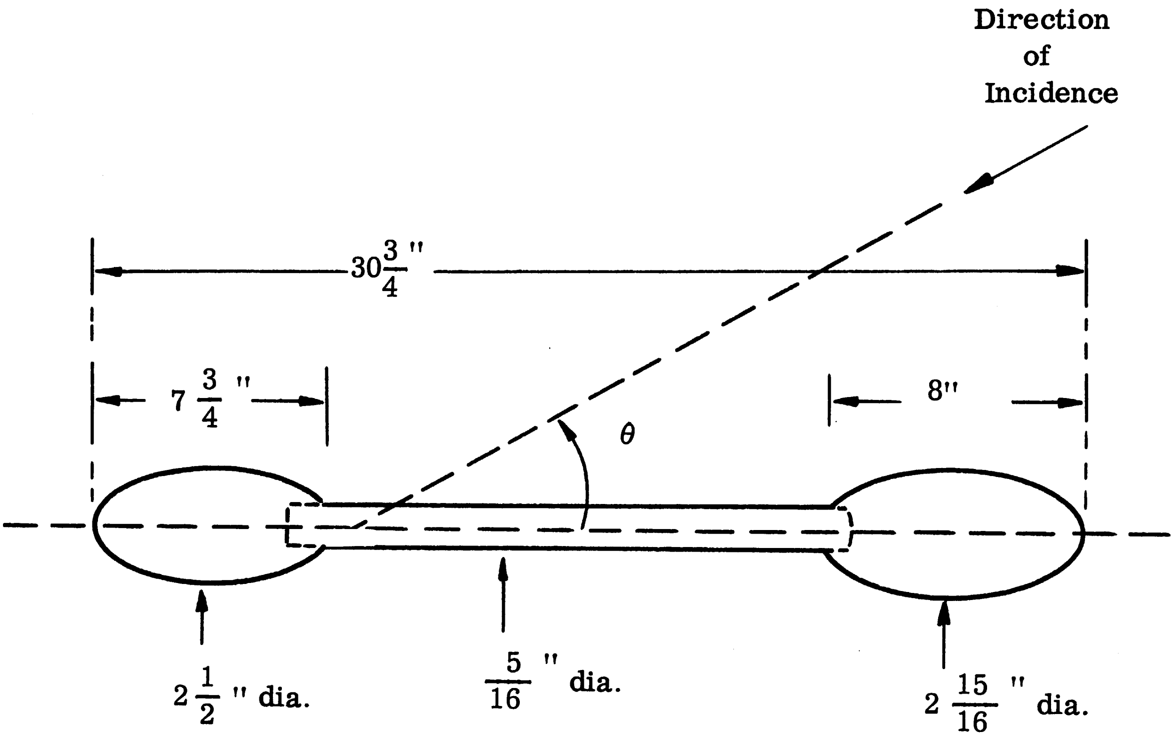

FIG. 4.2-6: SKETCH OF MODEL "C"
(dimensions are approximate)

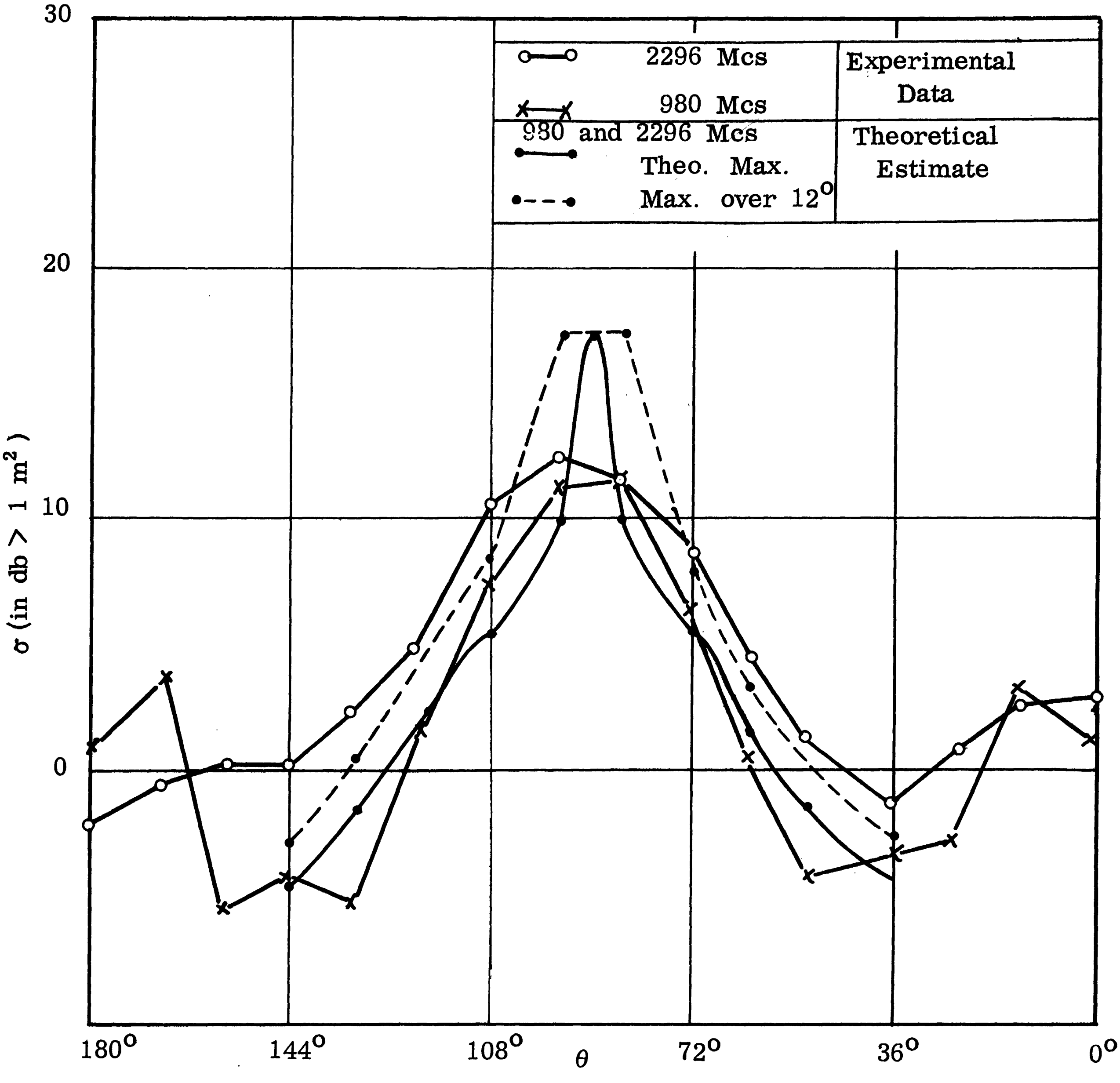

FIGURE 4.2-7: RADAR CROSS SECTION OF MODEL "C" AS A FUNCTION OF ASPECT AND FREQUENCY - FULL SCALE - MAXIMUM VALUES OVER 12° INTERVALS

The experimental data displayed peaks at (a) $\theta \approx 10^{o}$, (b) $\theta \approx 171^{o}$, (c) $\theta \approx 5^{o}$ and (d) $\theta \approx 176^{o}$.

Furthermore the nose-on and tail-on aspects according to theory should have nulls exhibited there at 980 mcs. Theory would predict null values of about -11 db relative to 1 m^2 at these aspects; the experimental data displayed values of -12.5 and -15 db for the nose-on and tail-on values respectively.

In the interval $36^{o} \leq \theta \leq 144^{o}$ a quick estimate of the theoretical maximum was obtained (by assuming all contributions were in phase); the theoretical curve resulting from this approach is also shown in Figure 4.2-7. This approach can be expected to serve well at predicting the "12^{o}-maxima" curve except at $\theta = 90^{o}$ where it is obvious that the cylinder contribution will not be "in phase" (necessarily) with the spheroid contributions. Thus, the fact that the theoretical estimate at $\theta = 90^{o}$ is a few db (about five) above the experimental maxima is not unexpected.

APPENDIX A

CROSS SECTION OF THE BOEING AIRPLANE, MODEL B

The cross section of the Boeing airplane (Model B as defined in the drawings provided by the Boeing Airplane Co.) has been calculated at the S-band frequency of 3000 mcs for the case of a horizontally polarized plane wave at aspects from nose-on to tail-on for a zero elevation angle. The airplane was broken up into a number of simple shapes and it was found that the various index numbers, $k\rho$, (where ρ is the critical dimension of the body-component) were sufficiently greater than one that physical optics methods could be used throughout.

The fuselage is represented by three prolate spheroids having slightly different dimensions and a truncated ellipsoid at the back. The exhaust section, which gives the chief body contribution at the tail-on aspect, is represented by an annular flat plate on the outside plus a cavity.

The main wing is represented by two flat ellipsoids which give the return from the leading and trailing edges. The small nose wing is modeled by flat plates which leads to thin wire type contributions for the aspects involved.

The air-intake is modeled at nose-on as another annular flat plate and a smaller circular flat plate representing the return from the interior of the intake. Near nose-on a cavity response was estimated. Near broadside the intake section looks most like a cylinder whose length, 48 inches, is the length of the specular line.

Finally the tail surfaces were represented by flat plates. The return from each surface was very large at broadside and about the same. The results plotted are due to a random phase combination. However, at S-band frequencies slight variations in wavelength or angle may cause large differences in phase and almost a 100 % increase or decrease in the contribution from the tail surface. (The tail surfaces were also modeled as truncated cones with considerable reduction in cross section.)

Multiple reflection considerations given to the cavities (air-intake and exhaust) and to the wing-fuselage combination indicated that relative peaks in these cross section contributions can be expected at particular aspect angles in the zero-elevation-angle plane. (These multiple-bounce contributions are due to geometry, not phase relations.) These critical angles were determined together with the expected maximum magnitudes. At some of these aspects these multiple-bounce contributions will dominate the return, thus we have attempted to bound the "average" or "random phase" estimate* of the cross section by summing all contributions other than the multiple-bounce ones for the lower bound and summing all contributions

---

*By definition this average or random phase cross section is given by $\sigma = \sum_{i=1}^{n} \sigma_i$ where σ_i is the cross section of the i^{th} component and there are n contributors.

including the envelope of the multiple-bounce ones for the upper bound. This gives bounds in the near nose-on and near tail-on aspect regions; an estimated range near broadside is obtained by employing the two different modelings of the tail surfaces mentioned above.

The resulting estimate of the cross section is shown in Figure A-1 with the expected location of relative peaks indicated. A model of this airplane was also tested experimentally at the simulated frequency of 2296 mcs. The theoretical approach would indicate that the returns at 2296 mcs and 3000 mcs should not differ by more than a factor of 1.3 at most aspects with a factor-difference of 1.7 possible at aspect normal to the vertical fine. (The 3000 mcs case being the higher at the relative peak locations.) Thus we can expect the 3000 mcs - theory curve to agree (on the average) to within about 2.5 db with the 2296 mcs experimental curve. Such a comparison is given in Figure A-2 where it can be observed that (1) the calculated range of values covers the experimental data quite well and (2) the prediction of the location of some of the relative peaks was quite successful.

The greatest apparent discrepancy between theory and experiment is in the vicinity of $\theta = 144^{o}$. This is due, in part, to slight differences in the two sides of the aircraft. The experimental data shown in Figure A-2 is for the right side of the aircraft; in Figure A-3 we display the data for the left side of the aircraft in the $180^{o} > \theta > 120^{o}$ region. It will be noted that the cross section tends to be larger (on the average) for the left side than the right side in the interval $132^{o} \angle \theta \angle 156^{o}$.

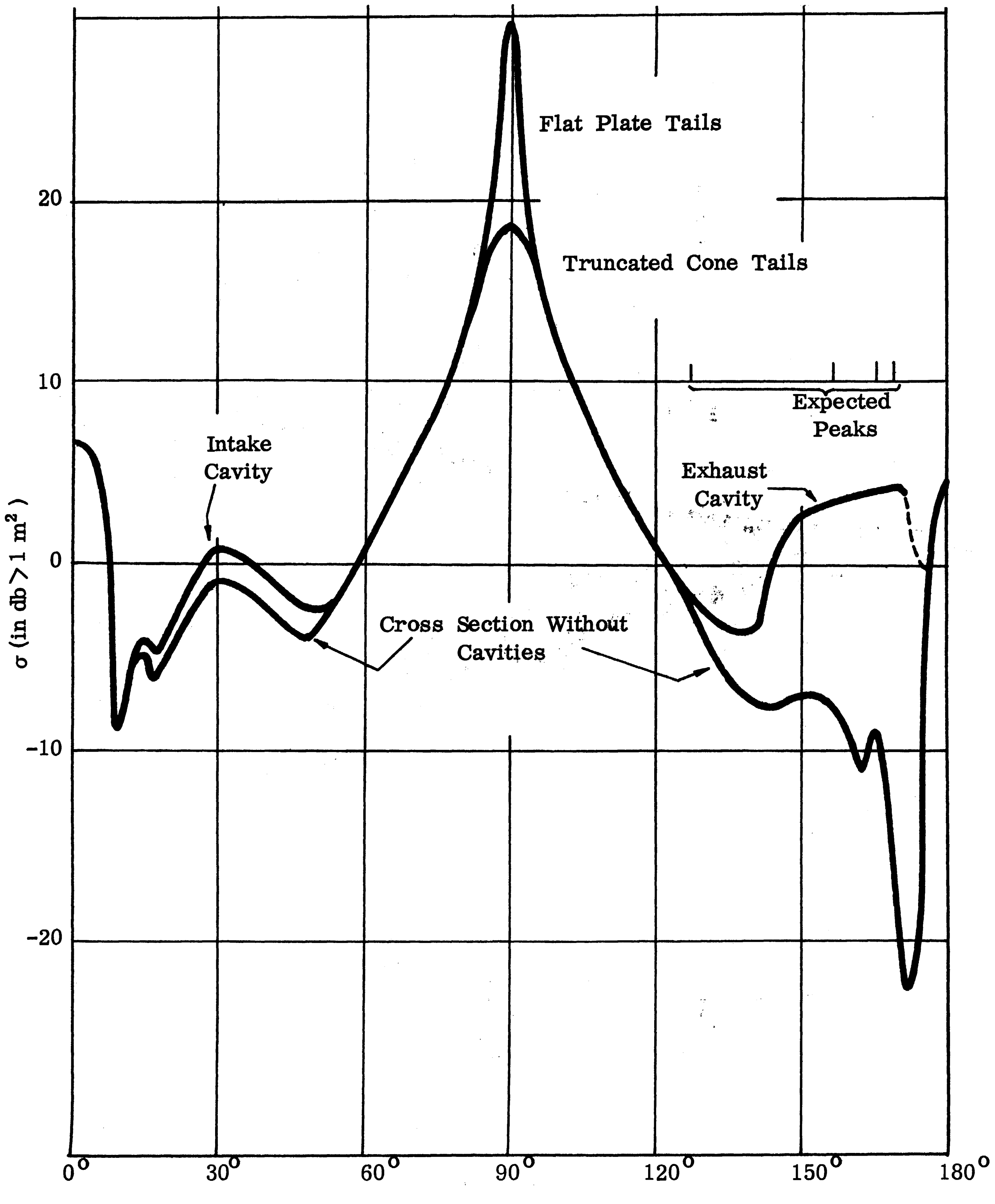

FIG. A-1: THEORETICAL S-BAND AVERAGE CROSS SECTION FOR FULL SCALE MODEL "B" AIRCRAFT

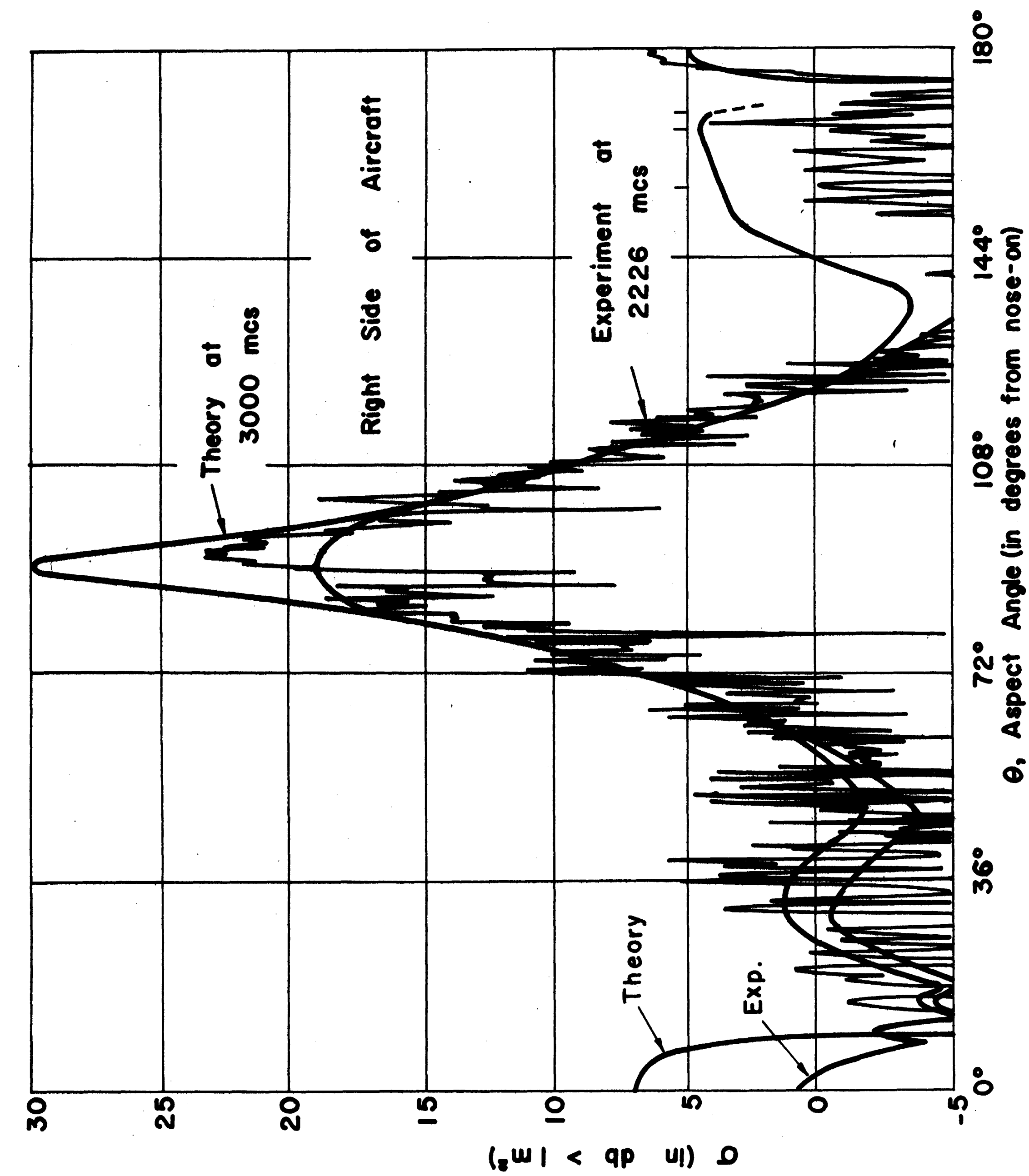

Fig. A-2. Comparison Between Theory and Experiment

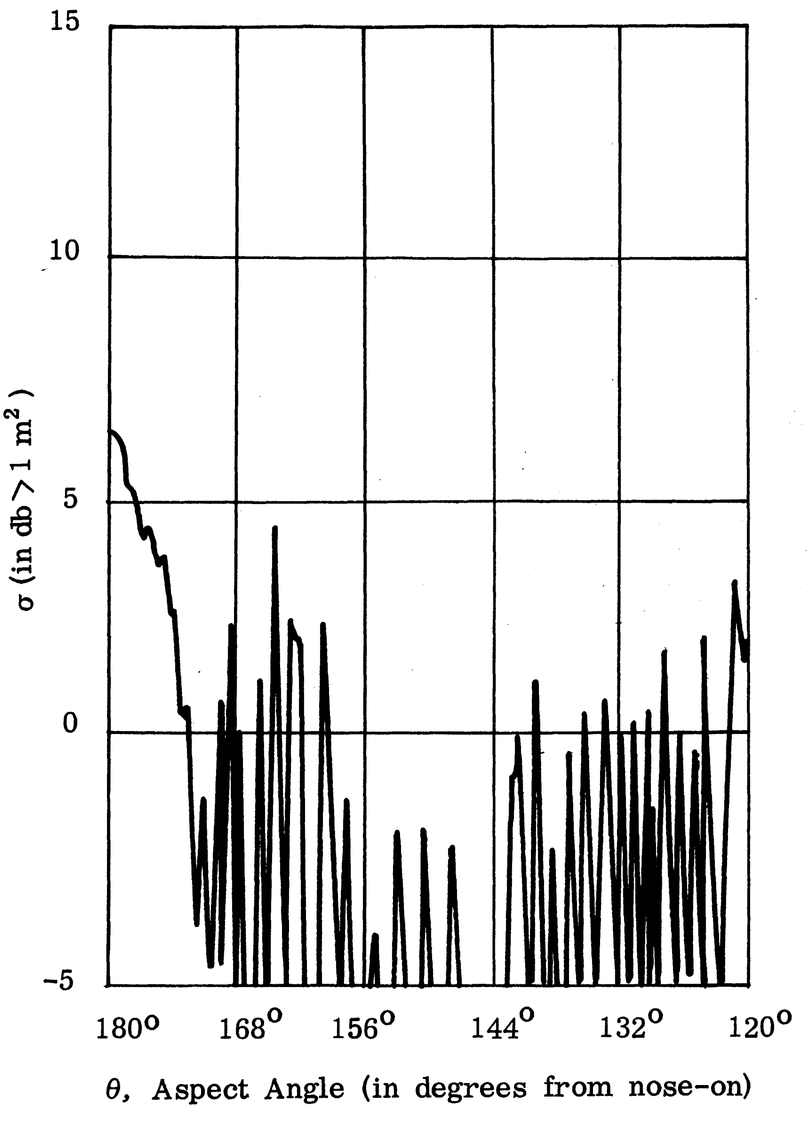

FIG. A-3: EXPERIMENTAL DATA FOR THE LEFT SIDE OF THE AIRCRAFT

REFERENCES

1. J.W. Crispin Jr., R.F. Goodrich, and K.M. Siegel, "A Theoretical Method for the Calculation of the Radar Cross Section of Aircraft and Missiles" University of Michigan Radiation Laboratory Report No. 2591-1-H (July 1959) UNCLASSIFIED.

2. R.E. Hiatt, "Radar Reflectivity of Mortar Shells" University of Michigan Radiation Laboratory Report 2862-1-F February 1959.

3. M.H. Cohen, "An Evaluation of some Aspects of Static Model Radar Echo Measurements" OSURF Report 475-17, June 1954, Contract AF 18 (600)-19